Supplementary Information for

Effect of Metallacarborane Salt H[COSANE] Doping on the Performance Properties of Polybenzimidazole Membranes for High Temperature PEMFCs

Jessica Olvera [a], Jorge Escorihuela [b,], Larissa Alexandrova [a], Andreu Andrio [c], Abel García-Bernabé [d], Luis Felipe del Castillo [a] and Vicente Compañ [d,]**

[a] Departamento de polímeros, Instituto de Investigaciones en Materiales, Universidad Nacional Autónoma de México (UNAM), Ciudad Universitaria, Apartado Postal 70-360, Coyoacán, Ciudad de México, 04510, México.

[b] Departamento de Química Orgánica, Universitat de València, Av. Vicente Andrés Estellés s/n, Burjassot 46100 Valencia, Spain.

[c] Departament de Física aplicada, Universitat Jaume I, 12080, Castelló, Spain.

[d] Departamento de Termodinámica Aplicada (ETSII), Universitat Politècnica de Valencia, Campus de Vera s/n. 46022 Valencia, Spain.

Table S1. Oxidative stability measured by weight loss evaluated by Fenton's test for PBI–1 membranes.

	Weight loss (%)		
H[COSANE] wt%	**After 12 h**	**After 24 h**	**After 96 h**
0	15	25	39
10	13	23	29
15	13	21	27
20	10	14	21
30	12	Break	Break

Table S2. Oxidative stability measured by weight loss evaluated by Fenton's test for PBI–1 membranes.

	Weight loss (%)		
H[COSANE] wt%	**After 12 h**	**After 24 h**	**After 96 h**
0	14	22	36
10	14	21	26
15	11	17	25
20	11	17	20
30	12	16	Break

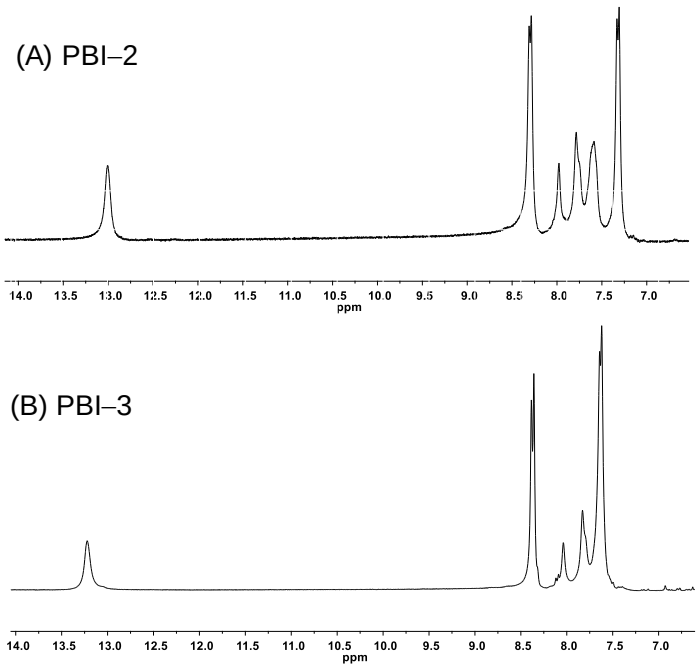

Fig. S1. ^{1}H NMR spectra in DMSO-d6 of synthesized (A) PBI–2 and (B) PBI–3.

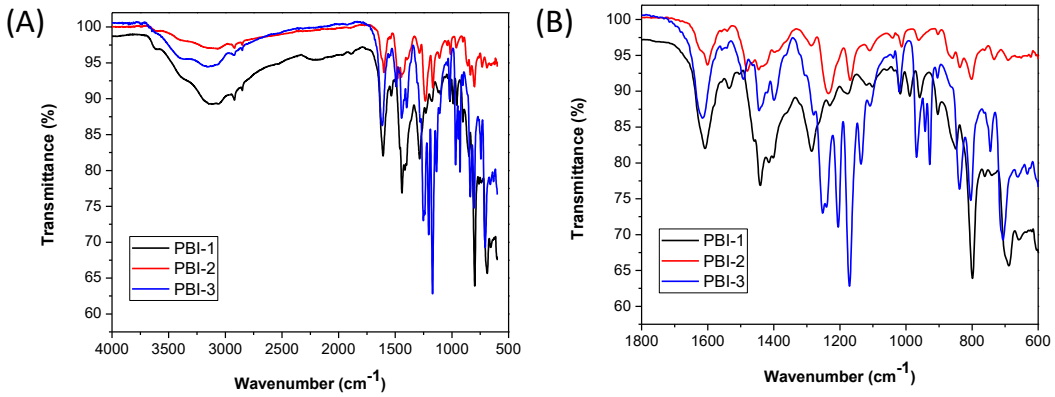

Fig. S2. (A) FTIR of PBI–1 (black line), PBI–2 (red line) and PBI–3 (blue line) and (B) fingerprint region of the spectra of the three PBI.

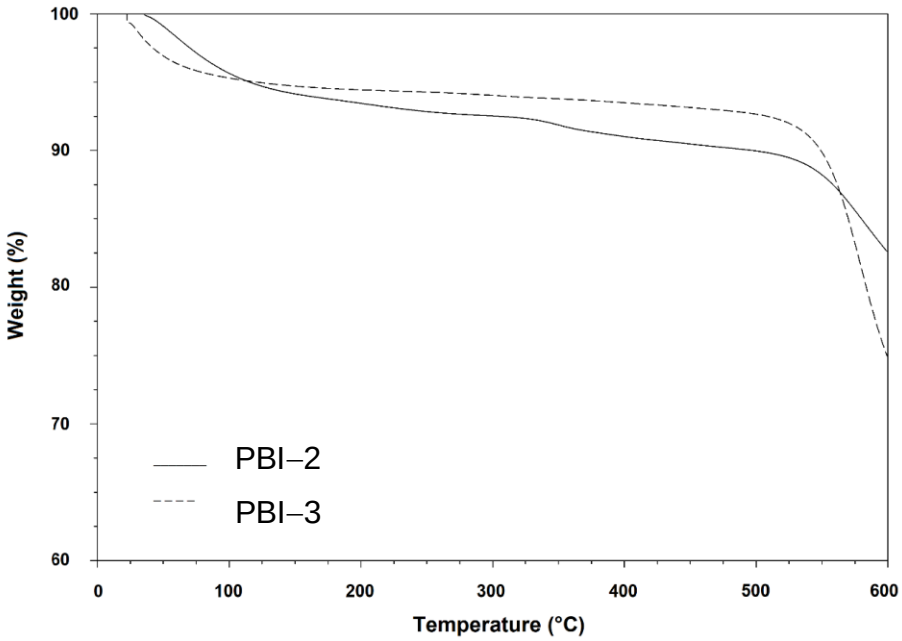

Fig. S3. TGA curves of synthesized PBI–2 and PBI–3 under a nitrogen atmosphere.

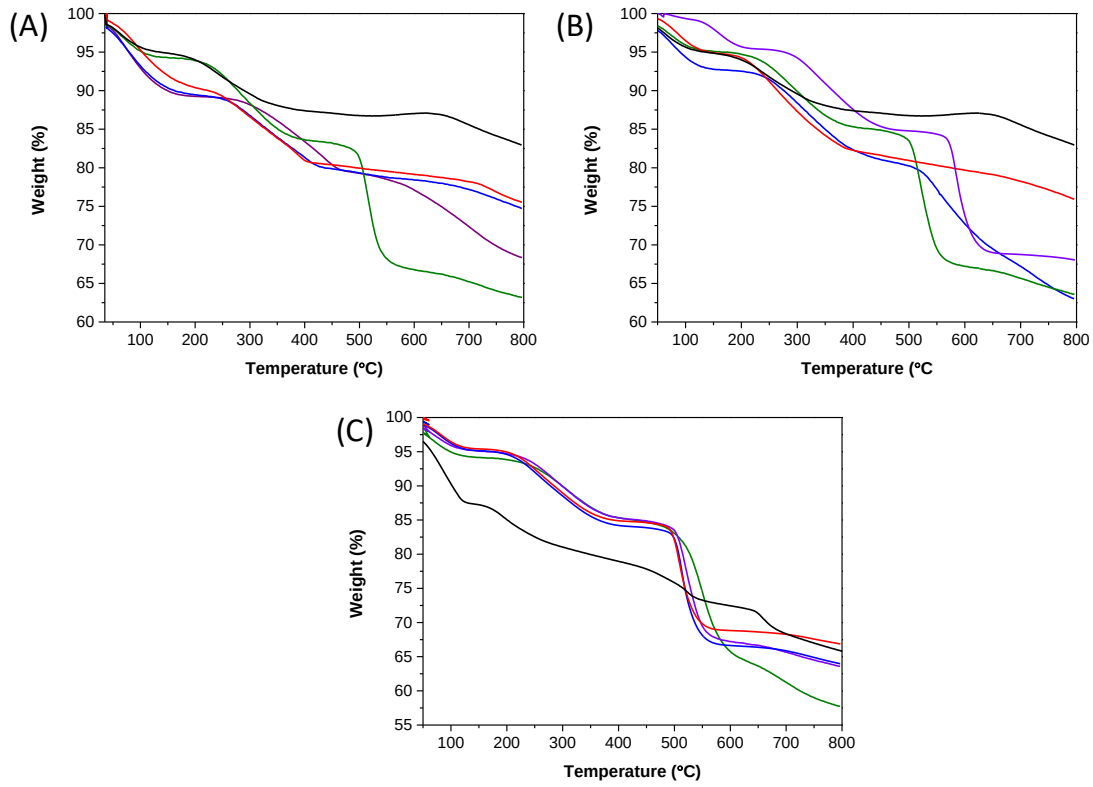

Fig. S4. Thermal stability of different composite membranes containing H[COSANE] at different concentrations 0 (——), 10 (——), 15 (——), 20 (——) and 30 wt % (——) for (A) PBI–1, (B) PBI–2 and (C) PBI–3.

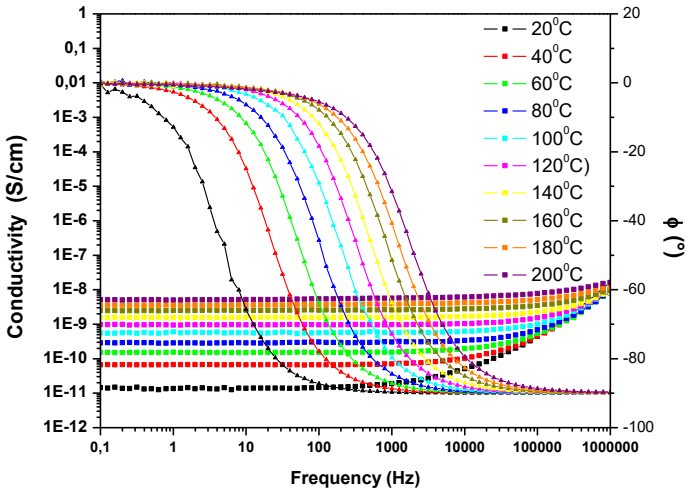

Fig. S5. Bode diagram for the conductivity of undoped composite membrane PBI-1-10H[COSANE] in the range of temperatures from 20 to 200 ºC.

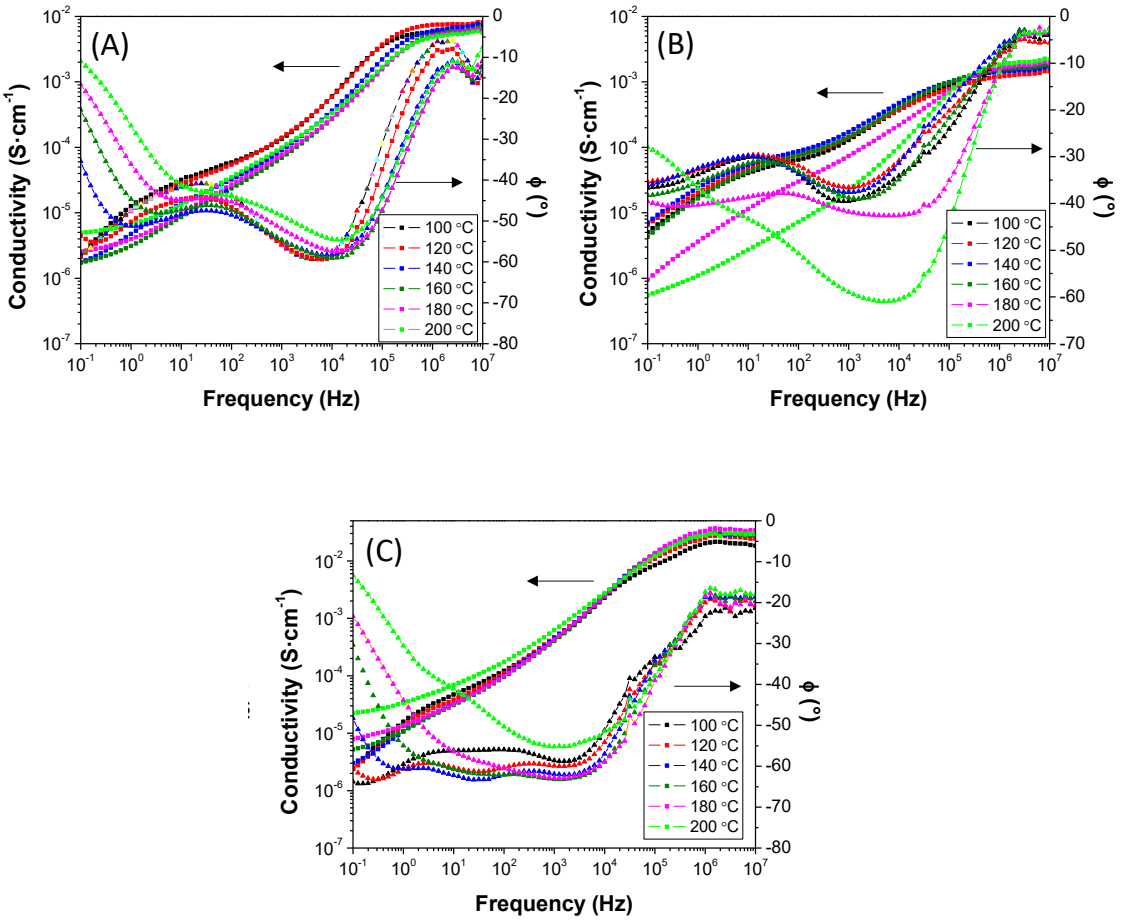

Fig. S6. Bode plots for PBI–1@15H[COSANE], PBI–2@15H[COSANE], and PBI–3@15H[COSANE] at different temperatures (100–200 °C).

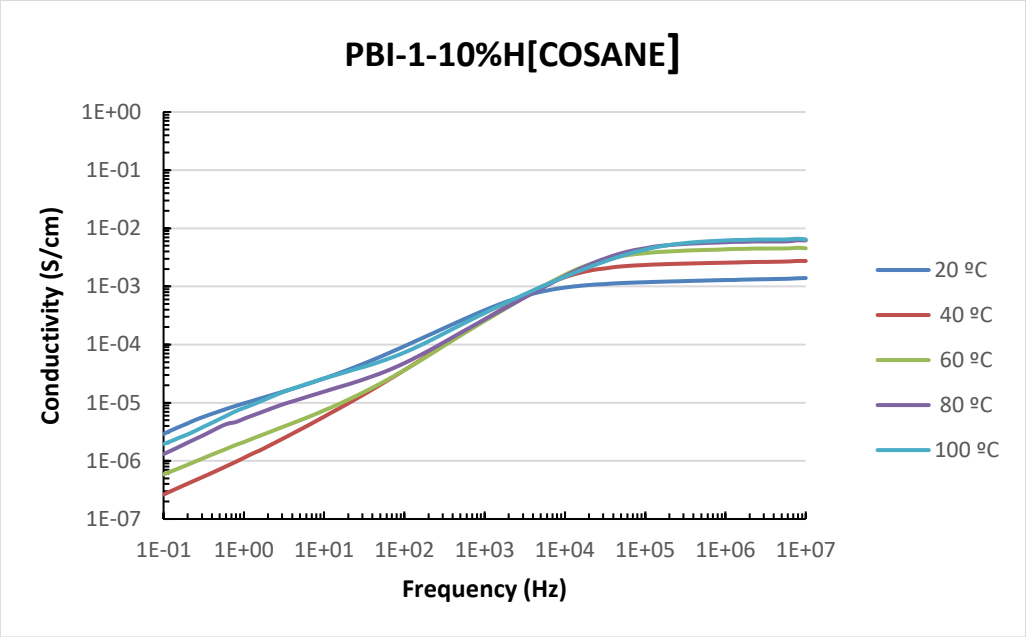

Fig. S7. Conductivity of doped (1 M H_3PO_4) composite membrane PBI-1-10H[COSANE] in the range of temperatures from 20 to 100 ºC.

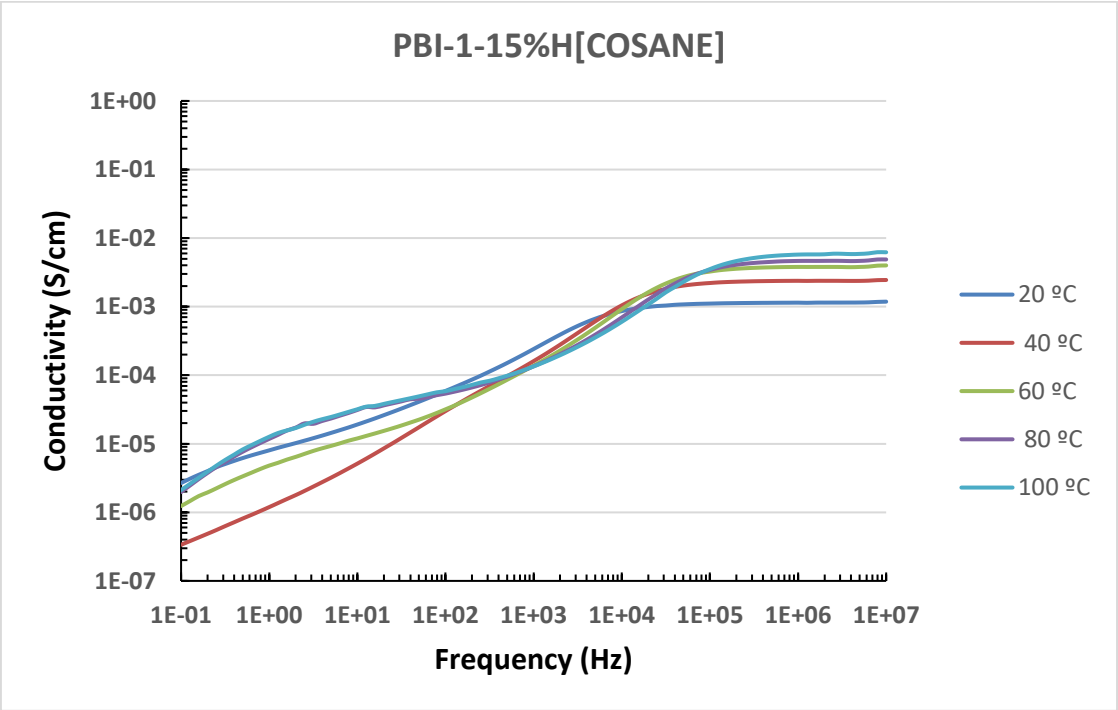

Fig. S8. Conductivity of doped (1 M H_3PO_4) composite membrane PBI-1-15H[COSANE] in the range of temperatures from 20 to 100 ºC.

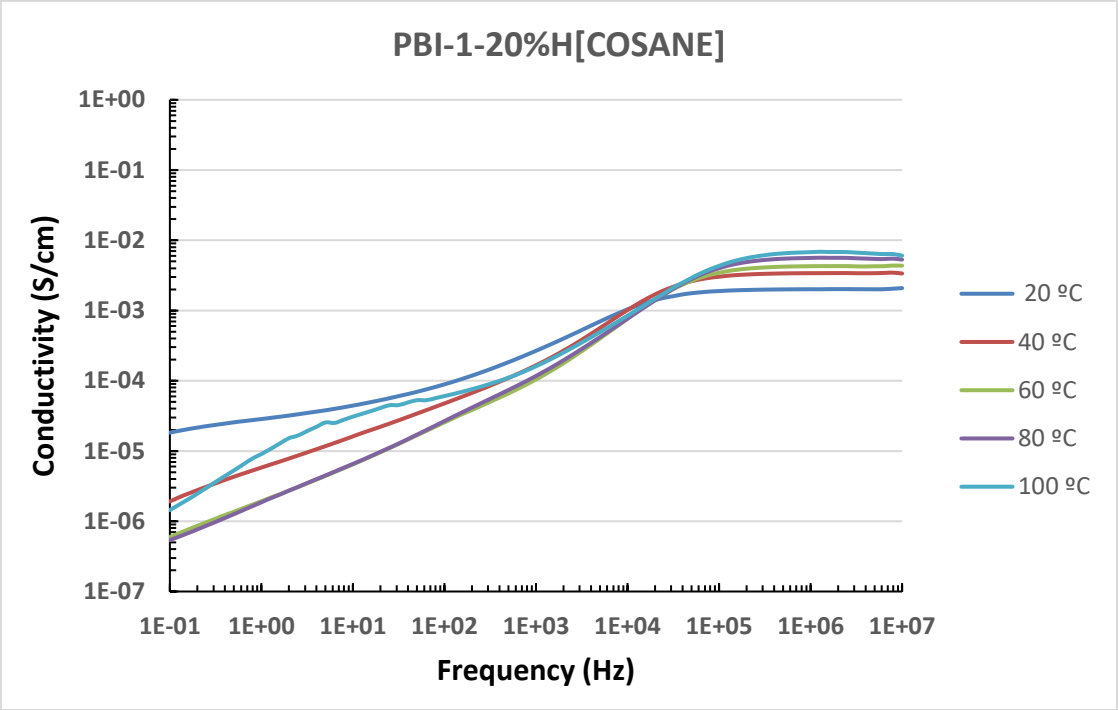

Fig. S9. Conductivity of doped (1 M H_3PO_4) composite membrane PBI-1-20H[COSANE] in the range of temperatures from 20 to 100 ºC.

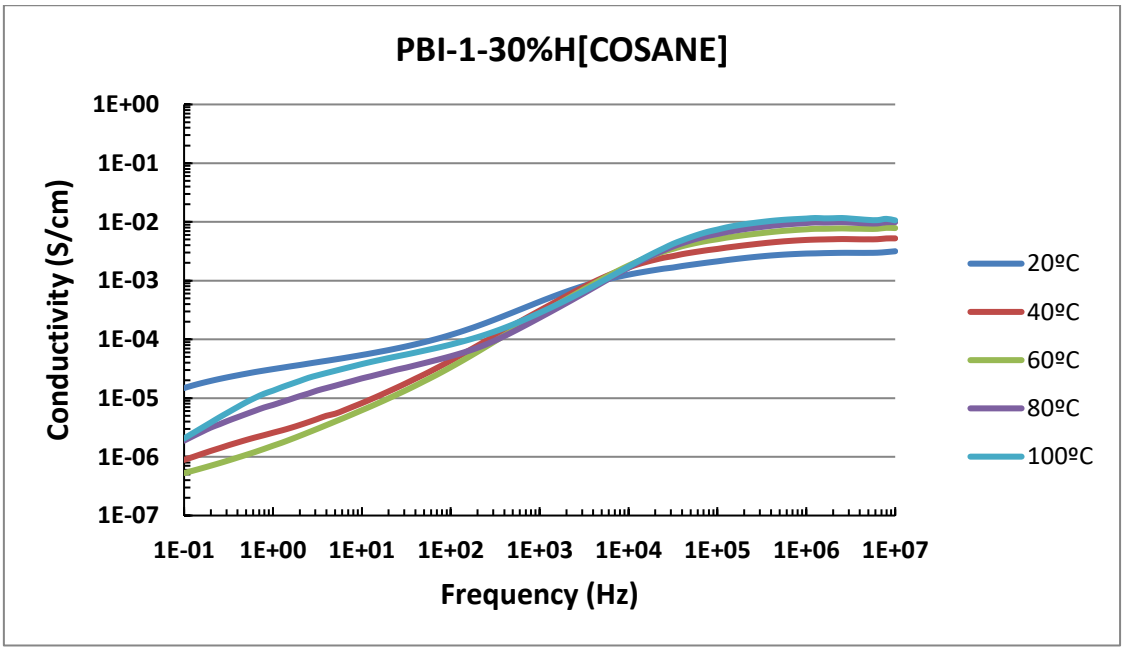

Fig. S10 Conductivity of doped (1 M H_3PO_4) composite membrane PBI-1-30H[COSANE] in the range of temperatures from 20 to 100 ºC.

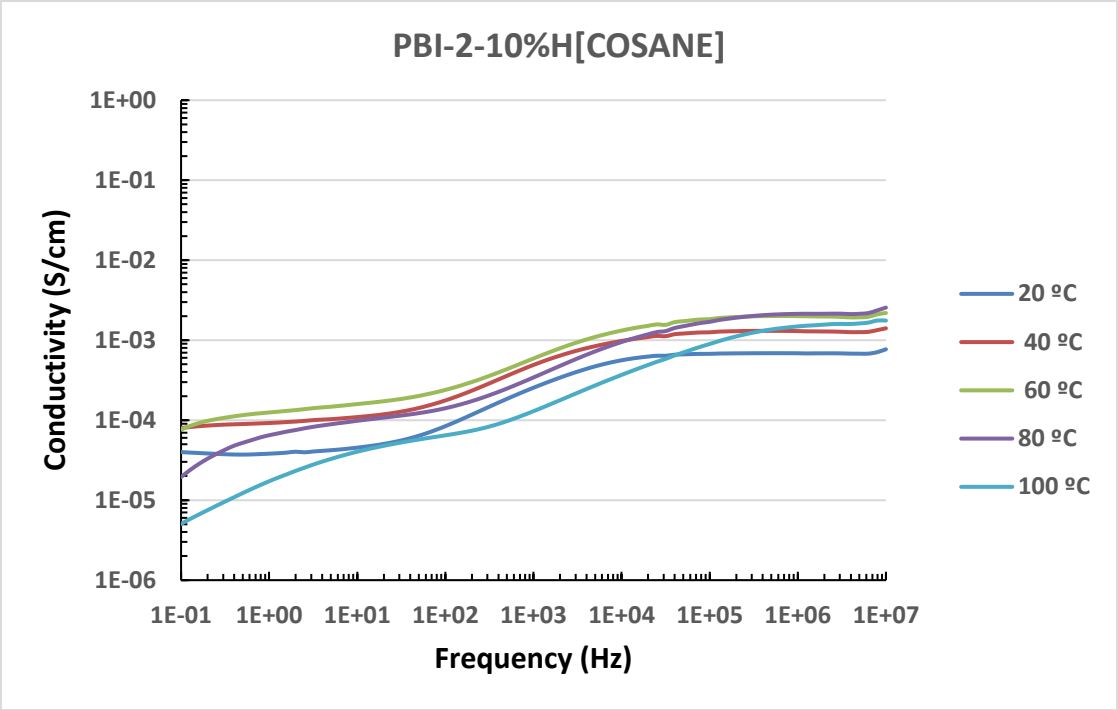

Fig. S11. Conductivity of doped (1 M H_3PO_4) composite membrane PBI-2-10H[COSANE] in the range of temperatures from 20 to 100 ºC.

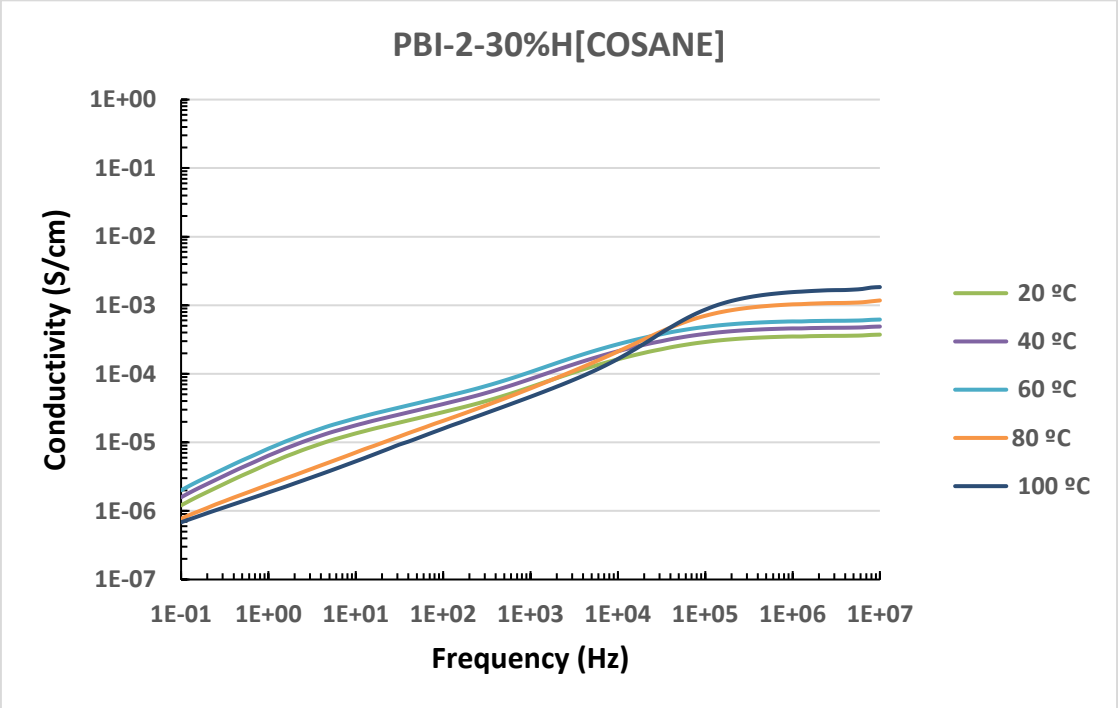

Fig. S12. Conductivity of doped (1 M H_3PO_4) composite membrane PBI-2-30H[COSANE] in the range of temperatures from 20 to 100 ºC.

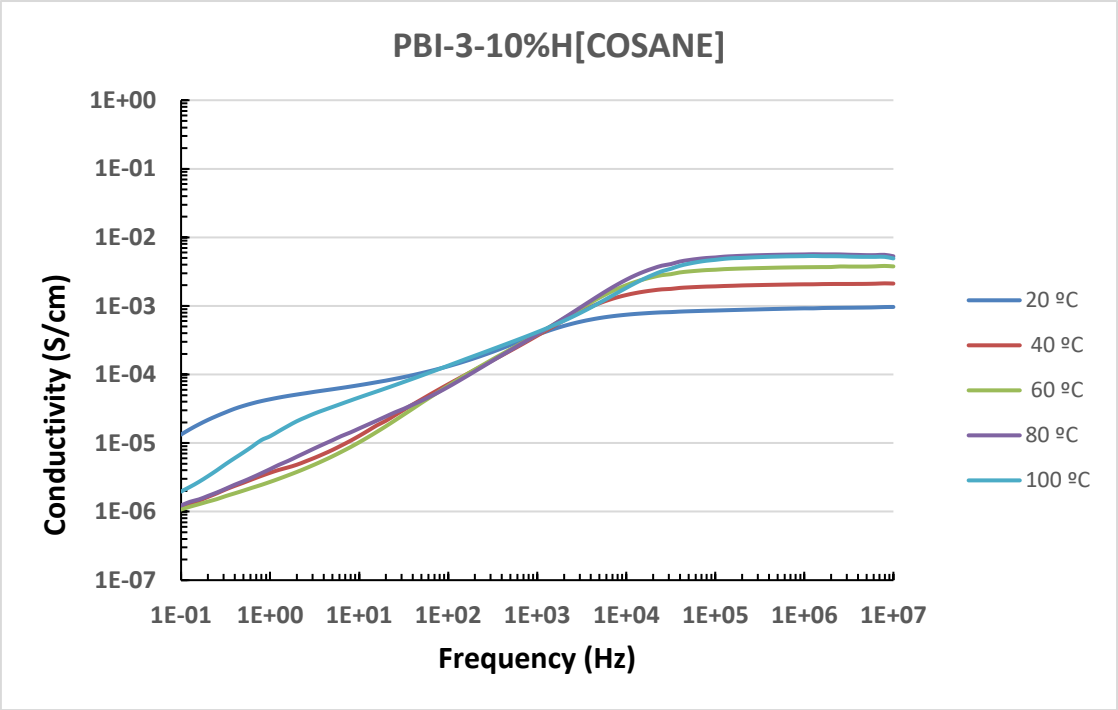

Fig. S13. Conductivity of doped (1 M H_3PO_4) composite membrane PBI-3-10H[COSANE] in the range of temperatures from 20 to 100 ºC.

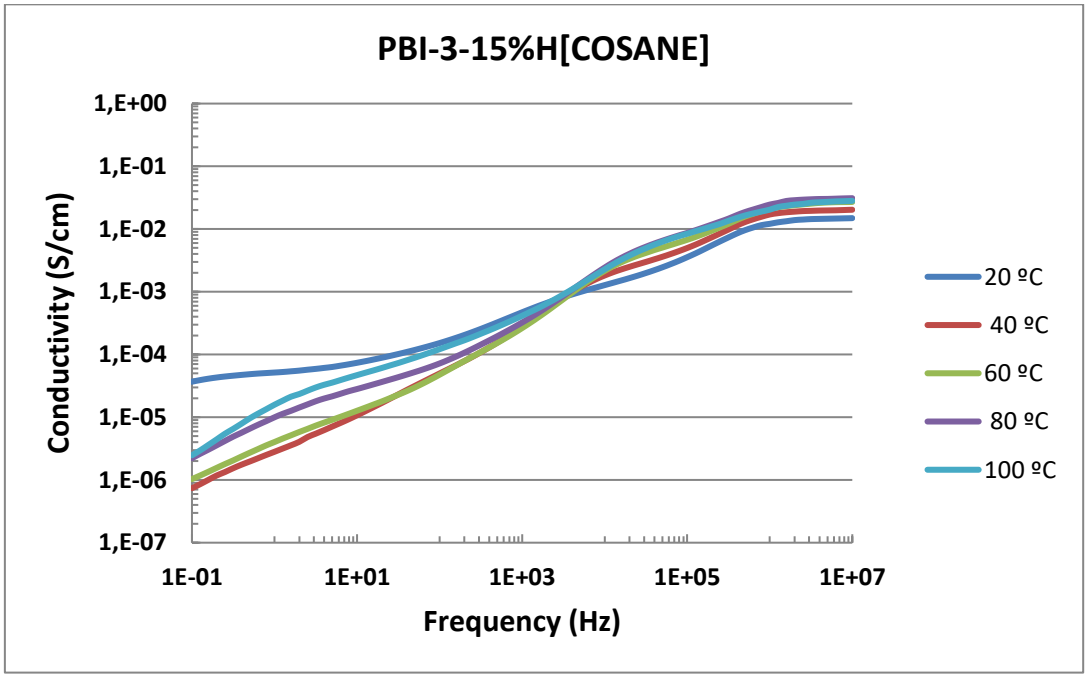

Fig. S14. Conductivity of doped (1 M H_3PO_4) composite membrane PBI-3-15H[COSANE] in the range of temperatures from 20 to 100 ºC.

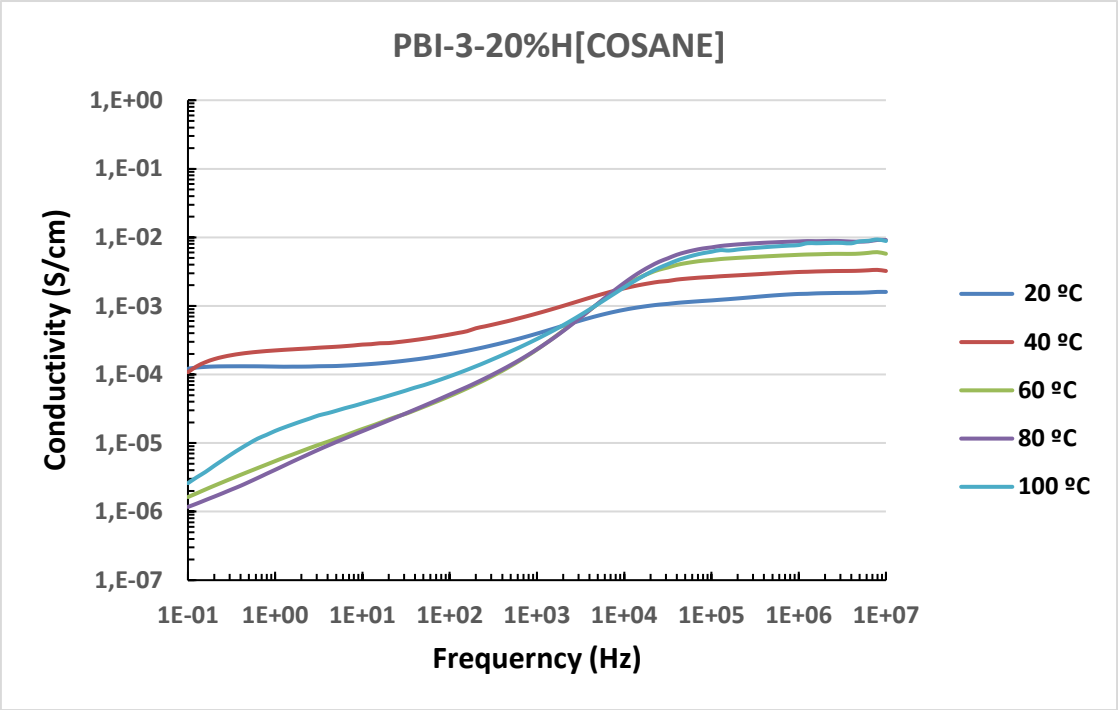

Fig. S15. Conductivity of doped (1 M H_3PO_4) composite membrane PBI-3-20H[COSANE] in the range of temperatures from 20 to 100 ºC.

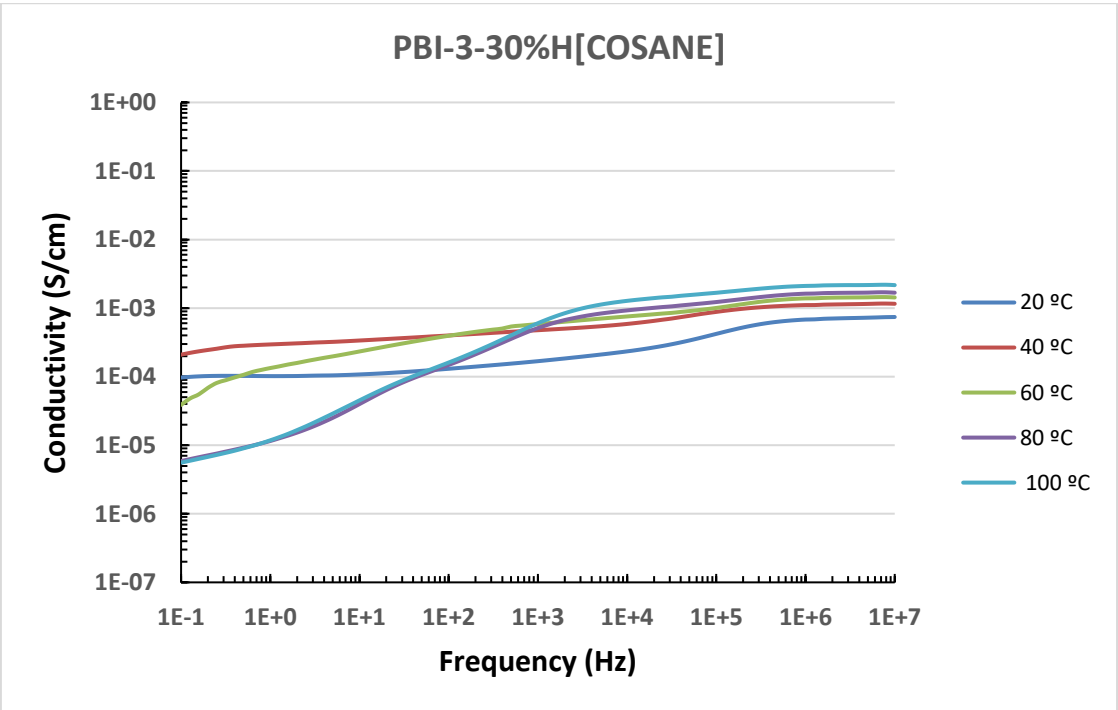

Fig. S16. Conductivity of doped (1 M H_3PO_4) composite membrane PBI-3-30H[COSANE] in the range of temperatures from 20 to 100 ºC.